ELSEVIER

Polymer 42 (2001) 9163–9172

polymer

www.elsevier.com/locate/polymer

The effect of end groups on thermodynamics of immiscible polymer blends. 2. Cloud point curves

Mark H. Lee[a], Cathy A. Fleischer[a,1], Ana Rita Morales[a,2], Jeffrey T. Koberstein[a,*], Ronald Koningsveld[b]

[a]*The Polymer Program and Department of Chemical Engineering, Institute of Materials Science, University of Connecticut, Storrs, CT 06269-3136, USA*
[b]*Polymer Institute Sigma Pi, Walderfeuchtstraat 13, 6132 HH Sittard, The Netherlands*

Received 22 March 2001; received in revised form 11 May 2001; accepted 11 May 2001

Abstract

The effect of chain end groups on the thermodynamics of polymer blends is investigated by the collection of cloud point curves for low molecular weight blends of poly(isoprene) (PIP) with three different α,ω-functionally-terminated poly(dimethyl siloxane) (PDMS) materials: α,ω-trimethylsilyl PDMS (PDMS–CH_3), α,ω-propylamino PDMS (PDMS–NH_2) and α,ω-propylcarboxy PDMS (PDMS–COOH). The cloud point curves for these blends differ radically, demonstrating the possibility of controlling miscibility of low molecular weight blends by modification of polymer chain ends. The apparent critical points for equivalent molecular weight blends of PIP/PDMS–CH_3, PIP/PDMS–COOH, and PIP/PDMS–NH_2 are found at temperatures of 250, 190, and 85°C, respectively, scaling inversely with the polarity of the PDMS end group. Cloud point curves, calculated from the Flory–Huggins (F–H) rigid lattice model and a quasi-binary extension of the F–H model, are in good agreement with the experimental cloud point data, and are used to estimate the interaction parameters for PIP/PDMS–CH_3 and PIP/PDMS–NH_2 blends. The interaction parameters for both blend types are found to be insensitive to the molecular weight of the PDMS component and to scale inversely with the polarity of the end group. The total interaction parameters for the PDMS–NH_2 blends are also calculated from the summation of binary interactions between blend components, PIP, PDMS, and end groups. Incorporation of amine end groups onto PDMS causes a decrease in the total interaction parameter calculated in this manner, consistent with the increased miscibility observed experimentally in blends containing PDMS–NH_2 in comparison to those containing PDMS–CH_3. In addition, the calculated binary interaction parameters show the following trend: $\chi_{DMS/NH_2} > \chi_{IP/DMS} > \chi_{IP/NH_2}$. This suggests that the observed compatibilization effect in blends with PDMS–NH_2 is driven by the repulsive nature of the interactions between the PDMS backbone and its end groups. © 2001 Published by Elsevier Science Ltd.

Keywords: Polymer blend phase diagrams; End group effects; Cloud point curves

1. Introduction

The development of new methods for the modification of polymer interfaces and for the compatibilization of immiscible polymer blends remains a topic of considerable academic and industrial interest. In a number of publications, our group has demonstrated that the modification of polymer end groups is a novel and practical means by which to accomplish these goals, and that there exists considerable promise that these ideas may be successfully adopted for commercial applications. These works have illustrated how end-functional polymers can be used effectively to modify the structure and properties of polymer surfaces [1–4], as well as the interfacial properties of polymer blends [5,6]. The latter work described how the interfacial tension between two immiscible homopolymer melts could be reduced by modification of the end groups on one of the homopolymers. More specifically, the interfacial tension for pseudo-binary blends of poly(butadiene) (PBD) with aminoalkyl-terminated poly(dimethyl siloxane) (PDMS–NH_2) was reduced by as much as 30%, as compared to blends containing methyl-terminated poly(dimethyl siloxane) (PDMS–CH_3).

In an attempt to explain this behavior, interfacial tension measurements were performed [6] on immiscible blends of

* Corresponding author. Present address: Department of Chemical Engineering and Applied Chemistry, Columbia University, MC4721, 500 W 120th Street, New York, NY 10027, USA. Tel.: +1-212-854-3120; fax: +1-212-854-3054.

E-mail address: jk1191@columbia.edu (J.T. Koberstein).

[1] Present address: Eastman Kodak Company, Rochester, NY 14650-2104, USA.

[2] Visiting Scientist from the Federal University of San Carlos, San Carlos, Brazil.

0032-3861/01/$ - see front matter © 2001 Published by Elsevier Science Ltd.
PII: S0032-3861(01)00399-8

PBD with mixtures of PDMS–CH_3 and PDMS–NH_2. The results of these measurements revealed that the aminoalkyl-terminated material did not exhibit significant interfacial activity, leading to the conclusion that the reduction in interfacial tension observed in the blends with PDMS–NH_2 cannot be attributed to a surfactant effect, but must rather be associated with changes in the bulk thermodynamics of the blends; the bulk interactions in the aminoalkyl-terminated blend must be more favorable than those of the methyl-terminated blends. Finally, it was proposed that this increased miscibility could be qualitatively explained within the framework of the binary interaction theory [7–9], which has been used by others to describe the phase behavior for random copolymer blends.

Only a few other previous studies [10–13] have considered the effects of end groups on the phase behavior of polymer blends. The latter two studies by Kuo and Clarson [12] and Qian et al. [13] examined the phase behavior (i.e. UCST cloud points) for blends of poly(methylphenylsiloxane) (PMPS) with PDMS. The end groups in these studies were α,ω-trimethylsilyl (CH_3) and α,ω-dimethylsilylsilanol (OH). Kuo and Clarson found that the interaction density parameters determined from analysis of the cloud point data did not change when the PDMS trimethylsilyl end groups were substituted with dimethylsilanol groups in blends with α,ω-trimethylsilyl PMPS. Qian et al. subsequently used a combination of the Flory–Huggins (F–H) lattice model with a temperature dependent interaction parameter and molecular simulation techniques to theoretically investigate the effect of end groups on the same PMPS/PDMS system for a variety of molecular weights and end group pairs (i.e. PMPS–OH/PDMS–OH, PMPS–CH_3/PDMS–CH_3, PMPS–OH/PDMS–CH_3, PMPS–CH_3/PDMS–OH). An extended binary interaction theory for polymer mixtures of two different end groups was utilized to account for the end group effects on the total blend interaction parameter. The results from the simulations indicated that the end groups and their fractions in low molecular weight polymer blends significantly affected χ interaction parameters and phase separation temperatures. At higher molecular weights, the end-group effects were not as significant. In studies of polyester–polycarbonate model blends by Kollodge and Porter [11], end group effects were successfully modeled using the binary interaction approach that was proposed previously by our group and is employed in the current paper.

In this paper, the phase behavior of similar pseudo-binary blend systems containing end-functional homopolymers is characterized in order to confirm suspected changes in their bulk interactions. The effects of end group type and molecular weight of the end-functional homopolymer on phase behavior are characterized by measuring cloud point curves on blends of poly(isoprene) (PIP) with PDMS–CH_3, PDMS–NH_2 and carboxyl-terminated poly(dimethyl siloxane) (PDMS–COOH). The experimental cloud point data are then modeled using several modifications of the F–H theory in order to estimate interaction parameters for the PDMS–CH_3 and PDMS–NH_2 systems. Lastly, the relationship between these interaction parameters and end group type are interpreted within the framework of the binary interaction theory, in order to elucidate the contributions of interchain and intrachain interactions to the overall blend miscibility.

2. Experimental

The PIP (Polymer Labs) and PDMS–CH_3 materials (Petrarch, methyl-terminated) employed in this study were used as received. The PDMS–NH_2 (Goldschmidt, aminopropyl-terminated) and PDMS–COOH (Goldschmidt, propylcarboxy-terminated) were synthesized by an equilibration reaction in which cyclic siloxane monomers are inserted into a difunctional precursor. The resulting polymers are, therefore, essentially guaranteed of having two terminal functional groups per chain [14]. Due to the nature of the polymerization reaction, the products are polydisperse, and contain a small amount of residual cyclics. The PDMS–NH_2 materials were subsequently fractionated by supercritical fluid chromatography [15] in order to obtain materials of narrower molecular weight distribution that were free of cyclics.

The molecular weights and molecular weight distributions of the PDMS materials were characterized by size exclusion chromatography (SEC), vapor phase osmometry (VPO) and end group titration (EGT). The utilized techniques and procedures are described fully in the previous article of this series [6]. The characteristics of the polymers employed in the current study are summarized in Table 1. For clarity, the sample designations include the mean of the number-average molecular weights from VPO and EGT analyses, and the identity of the end group. The densities (at 30.0 ± 0.1°C) of PDMS oligomers were determined using a densitometer (Anton Paar model DMA60 and model 602 external cell) in order to calculate the volume of the end groups.

Cloud points were measured by laser light scattering using an apparatus constructed in-house. The laser (1 mW, Melles Griot, He–Ne) was directed through 1 mm channels cut into a heating block and onto the sample, which was held in a glass tube at the center of the heating block. The glass tube also contained a thermocouple and was stirred under vacuum throughout the experiment. The scattered light was detected using a photomultiplier tube oriented at an angle of 45° with respect to the incident light. The specimens were heated at a constant rate, during which the temperature dependence of the scattered light intensity was measured.

Polymer blends were prepared by adding a known amount of each polymer into the glass tube using calibrated 100 ml positive displacement syringes (Drummond). Subsequent samples of different concentrations were prepared by the addition of more PDMS to the original mixture in the

Table 1
Material characteristic as determined by vapor phase osmometry (VPO), size exclusion chromatography (SEC), and end group titration (EGT). Reported errors indicate one-half the range of values for two to three measurements

Sample designation	End group	M_n-VPO	M_n-EGT	M_n-SEC	M_w/M_n-SEC
PDMS-890–CH_3	Methyl	893±156	n/a	n/a	1.10
PDMS-1120–CH_3	Methyl	1120±37	n/a	n/a	2.22
PDMS-1270–CH_3	Methyl	1270±110	n/a	n/a	1.17
PDMS-860–NH_2	Propylamine	845	876±6	280	2.19
PDMS-990–NH_2	Propylamine	970±320	1010±10	393	2.46
PDMS-1310–NH_2	Propylamine	n/a	1310±16	410	2.28
PDMS-1390–COOH	Propylamine	1310	1470	1210	2.90
PIP	–	n/a	n/a	1250	1.07

glass tube. Blends were cooled from above the cloud point at rates of 2, 1 and 0.5°C/min and the cloud point was determined by extrapolation of these sets of data to an infinitely slow cooling rate. Theoretical phase diagrams, for both binary and quasi-binary systems, were calculated using programs developed in-house specifically for the current PIP/PDMS blend systems. The program calculates the cloud point curves by equating the chemical potentials of the coexisting phases (two for binary, three for quasi-binary) derived from the original F–H rigid lattice theory [16] and the modified F–H theory accounting for the quasi-binary phase behavior, described elsewhere in detail by Koningsveld et al. [17–19].

In order to compare the experimental interaction parameters quantitatively, it is essential to employ the same reference volume in regressing cloud point data for all of the blends. Normally, one defines the reference volume as the smallest monomer volume. In the present case however, where the solubility parameter of the end group is to be calculated using group additivity concepts, we set the reference volume in both binary and quasi-binary models equal to that of the dimethylsilylpropylamine end group. This ensures that the end group occupies one lattice site so that its solubility parameter may be calculated. If the end group were to occupy more than one lattice site, each end group lattice site would differ in chemical constitution and it would be necessary to treat the blend as a four-component system with six binary interaction parameters. All relative molar volumes, normalized chain lengths and interaction parameters were therefore calculated with respect to a reference volume given by the dimethylsilylpropylamine end group (128 cm^3/mol).

The binary model incorporated a temperature dependent expression for the F–H interaction parameter, χ_{AB}, defined as:

$$\chi_{AB}(T) = \chi_S + \frac{\chi_H}{T} \quad (1)$$

where T is the absolute temperature. Experimentally, it was found that the entropic contribution to the overall interaction parameter was very small in magnitude (of the order of 0.01) and it was therefore neglected when regressing the models to experimental cloud point data. The models were regressed to cloud point data by minimizing the sum of residual squared errors.

It has been observed in the literature that both the location of the critical point and the interaction parameter for binary blends vary with the molecular weight and molecular weight distribution of the components [20–22]. The theoretical effects of molecular weight and its distribution on binary phase diagrams have also been discussed [23,24]. Although many different approaches have been utilized till date in order to model cloud point curves exhibiting 'apparent' double critical points, as in our data, the vast majority of the techniques involve fitting the curves with parameters of little physical significance. It was the objective of the authors in the current paper to utilize models that were capable of representing the experimentally observed cloud points well while maintaining the theoretical basis of the models.

The F–H model modified for the quasi-binary behavior, as utilized by Koningsveld et al. [19], is used in the current study to account for the effect of the entire molecular weight distribution of the end-functional PDMS components on the overall phase behavior of the blend more fully. The approach considers a polydisperse polymer as a mixture of two monodisperse fractions, as a zero order approximation. The cloud point curve is then calculated by taking a quasi-binary section of the multidimensional temperature–composition ternary phase diagram. A more complete description of the calculation method, and the pertinent equations, are provided in Appendix A. This method yields much better correlation between the model calculations and the experimental cloud point data, for the blends containing the polydisperse PDMS–NH_2 components, than when an extension of the F–H theory in which a concentration-dependent χ_{AB} [25–27] is used. As a result, only the modeling results from the quasi-binary extension are presented in this paper.

3. Results and discussion

The effects of end group type on the bulk interactions and phase behavior of immiscible blends were characterized by measuring the cloud point curves on model blends of PIP

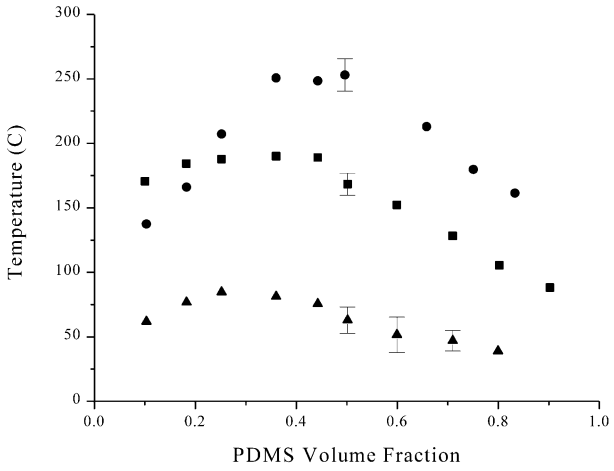

Fig. 1. Experimental cloud point curves: PIP/PDMS-1120–CH_3 (filled circles), PIP/PDMS-1390–COOH (filled squares), PIP/PDMS-990–NH_2 (filled triangles). Representative error bars are included with some of the data points.

with PDMS. PDMS homopolymers of similar chain length, but with three different end groups were employed for this purpose: PDMS-1120–CH_3 (methyl-terminated), PDMS-1390–COOH (carboxyl-terminated), and PDMS-990–NH_2 (amine-terminated). The results are shown in Fig. 1. All three systems exhibited phase behavior of the upper critical solution temperature (UCST) type, suggesting that the bulk interactions between blend components are repulsive in nature. Two effects are evident in these data. First, the apparent critical temperatures, T_c^{app}, for the blends appear to be dependent upon the identity of the PDMS end group, such that $T_c^{app}{}_{CH3} > T_c^{app}{}_{COOH} > T_c^{app}{}_{NH2}$. This trend suggests an inverse relationship between the polarity of the PDMS end group and the apparent critical temperatures. Secondly, there is a shift in the apparent critical composition toward lower PDMS content with increasing end group polarity. For the oligomers employed in this initial study (i.e. the nominal molecular weights employed were about 1000 Da), the apparent critical temperatures shift by as much as 165°C when more polar end groups are incorporated into the chain architecture.

The effects of molecular weight on the blend phase behavior were also investigated using blends of PIP with two sets of PDMS–CH_3 and PDMS–NH_2 homopolymers. The results are illustrated in Fig. 2. Examining first the cloud point curves for the two PIP/PDMS–CH_3 blends (open symbols), an increase in the apparent critical temperature is evident with increasing PDMS molecular weight. This is consistent with the expected decrease in combinatorial entropy in systems of higher molecular weight. Within the experimental error, the qualitative features of the two curves appear to be nearly identical. The apparent critical compositions for the PIP/PDMS–CH_3 blends are observed at volume fractions of about 0.5, which is consistent with the theoretical expectations for blends of two homopolymers of approximately equal length.

Qualitatively, similar phase behavior is observed for the PIP/PDMS–NH_2 blends of different molecular weights (filled symbols): lower molecular weights of PDMS yield lower apparent critical temperatures and the overall shape of the curves is independent of the molecular weight. However, unlike with the PIP/PDMS–CH_3 blends, the apparent critical compositions are shifted toward lower PDMS concentrations. A comparison of phase behavior of PIP/PDMS–CH_3 and PIP/PDMS–NH_2 blends, of similar molecular weight, reveals significant differences: the apparent critical temperatures are lower and the apparent critical compositions appear shifted toward lower PDMS concentration for the PIP/PDMS–NH_2 blends. The addition of amine end groups onto PDMS homopolymer, the latter represented by the analogous PDMS–CH_3 in the current study, shifts the apparent UCST from 205 (for PDMS-1270–CH_3) to 184°C (for PDMS-1310–NH_2), and from 121 (for PDMS-890–CH_3) to 73°C (for PDMS-860–NH_2). The greater shift observed in the UCST of blends of lower molecular weight is due to the higher end group concentration in these blends. The shift in the apparent critical concentration is also correlated with the end group concentration, as the lower molecular weight blend displays a larger shift toward lower PDMS concentration. Thus, it can be stated from these results that a change in the end group type has a pronounced effect on the intrinsic phase behavior of blends, at least on a qualitative level.

In an attempt to quantitatively explore the changes in phase behavior observed with different end groups, the cloud point data for the PIP/PDMS–CH_3 blends were modeled using the F–H theory [16] while data for the PIP/PDMS–NH_2 blends were modeled with a modified F–H theory, incorporating quasi-binary phase behavior [19], respectively. The quasi-binary approach, in the current study, was utilized to better model the effects of polydispersity evident in the cloud point curves of PIP/PDMS–NH_2 blends, in which the PDMS–NH_2 components had values of

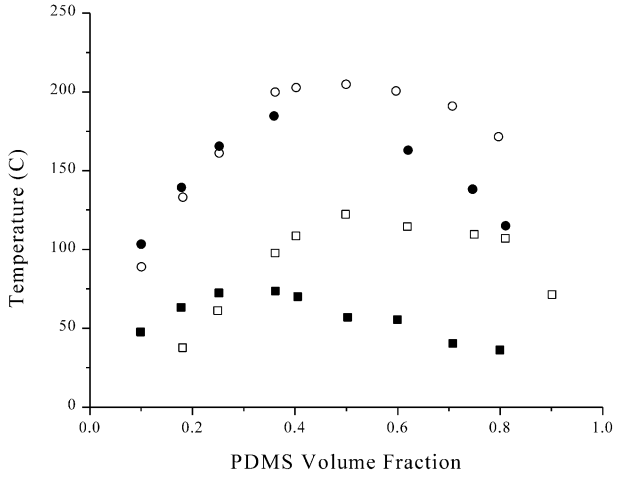

Fig. 2. Experimental cloud point curves: PIP/PDMS-1270–CH_3 (open circles), PIP/PDMS-1310–NH_2 (filled circles), PIP/PDMS-890–CH_3 (open squares), PIP/PDMS-860–NH_2 (filled squares).

M_w/M_n above 2. This effect is particularly pronounced in the lower molecular weight blends.

It was found by Koningsveld et al. [19,25] that the true critical point of liquid–liquid multicomponent polymer solutions was found to be located on the right-hand branch of the cloud point curve, often accompanied by a depression at its location. In addition, the specific features of this depression were shown to be largely dependent on the details of the molecular weight distribution, with the depression deepening with increasing M_z/M_w at constant M_w/M_n. This lends justification to using a quasi-binary model to more accurately predict the phase diagrams of blends with the polydisperse PDMS–NH_2 components, which exhibit apparent double critical points. The quasi-binary approach splits the polydisperse blend component (designated component 2) into two new monodisperse fractions (species 2a and 2b) and better incorporates the effect of the entire molecular weight distribution by using number-average, weight-average and z-average molecular weights (M_n, M_w, and M_z respectively) in calculating the phase diagram.

The true critical compositions and the corresponding critical temperatures (ϕ_c and T_c, respectively) were calculated from the binary and quasi-binary models for the PIP/PDMS–CH_3 and PIP/PDMS–NH_2 blends, respectively and are shown in Table 2 and in Figs. 3–6 (marked by ×). It should be remembered that the 'apparent' critical point, approximated to be at the highest temperature of the UCST cloud point curve, is not necessarily the true critical point. The latter has a strict thermodynamic definition which is mathematically expressed as $(\delta^3\Delta G/\delta\phi_2^3)_{P,T} = 0$ for binary systems and as Eqs. (A13) and (A14) in Appendix A for quasi-binary systems. For the PIP/PDMS–CH_3 blends, the critical points coincide with the highest points of the UCST curve, consistent with the inherent assumption in the F–H model of a strictly binary mixture. The PIP/PDMS-1270–CH_3 blend results in ϕ_c of nearly 0.5, which is expected since the molecular weights of PIP and PDMS components of the blend are nearly identical. For the PIP/PDMS–NH_2 blends, the critical points coincide roughly with the depression in the cloud point data, as was observed by Koningsveld et al. in their studies of multicomponent polymer solutions. This depression is more pronounced in the PIP/PDMS-860–NH_2 blend and as a result, the overall fit appears qualitatively better than that of the PIP/PDMS-1310–NH_2 blend. This trend is likely caused by the fact that molecular weight distribution effects are greater for lower molecular weight systems. In addition, with end-functional systems in particular, this effect may increase dramatically since end group concentrations are much higher in the lower molecular weight blends.

Table 2
Critical points determined graphically (denoted 'apparent') and from model calculations for PIP/PDMS blends. All volume fractions are with respect to the end function PDMS component and all temperatures are in °C

Blend	ϕ_c	T_c	T_c^{app}
PIP/PDMS-1270–CH_3[a]	0.50	201	205
PIP/PDMS-1310–NH_2[b]	0.45	145	184
PIP/PDMS-890–CH_3[a]	0.54	122	121
PIP/PDMS-860–NH_2[b]	0.51	64	73

[a] Calculated from the binary F–H model with a temperature-dependent interaction parameter.
[b] Calculated from the F–H model with quasi-binary modification and with a temperature-dependent interaction parameter.

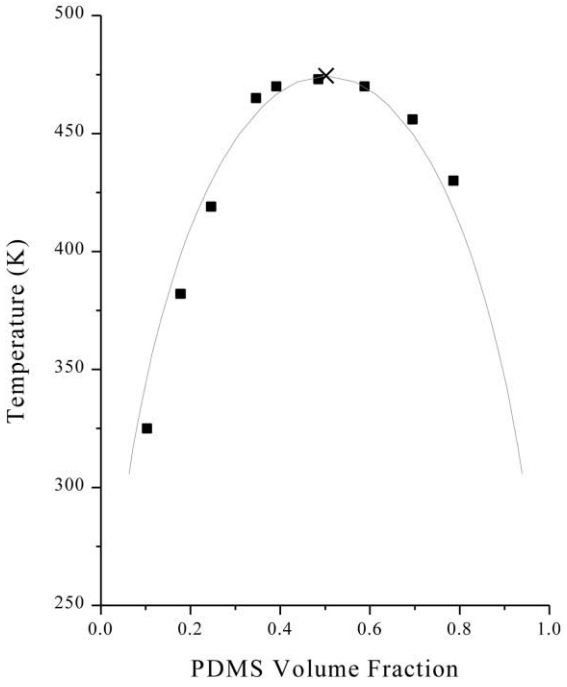

Fig. 3. PIP/PDMS-1270–CH_3 cloud point curves: experimental (squares), binary model (line), critical point (×).

The experimental cloud point data and the model fits for the PDMS–CH_3 and PDMS–NH_2 blend systems are presented in Figs. 3–6. The corresponding interaction parameters at 30°C are given in Table 3. All model fits appear to correspond well with the experimental cloud point data. It is worth noting that in all the four model fits, the sole adjustable parameter is the temperature dependent interaction parameter, χ_H, which can be directly determined from the temperature dependence of the cloud point envelope. The experimental interaction parameters in Table 3 show two qualitative trends. First, within the error of the cloud point data, the interaction parameters for blends having the same end group are not dependent on the molecular weight, at least in the systems used in the current study. Secondly, the interaction parameters for the PIP/PDMS–NH_2 blends are significantly lower than those for the PIP/PDMS–CH_3 blends, as expected for blends with lower UCST. These results confirm our previous conclusion [6] that the lower interfacial tensions observed for the PIP/PDMS–NH_2 blends are attributable to more favorable overall bulk interactions in the blend as the end group is changed from a methyl to an amine.

The interaction parameters, determined by regressing the

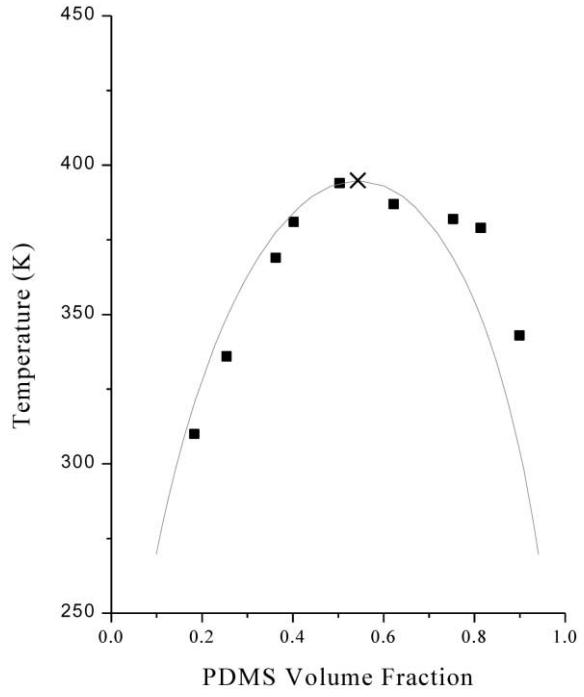

Fig. 4. PIP/PDMS-890–CH_3 cloud point curves: experimental (squares), binary model (line), critical point (×).

models to the experimental cloud point data, clearly demonstrate that modification of PDMS chains with polar functional end groups generally increases miscibility with PIP. Experimental interaction parameters for PIP/PDMS–NH_2 blends were found to be significantly lower than those

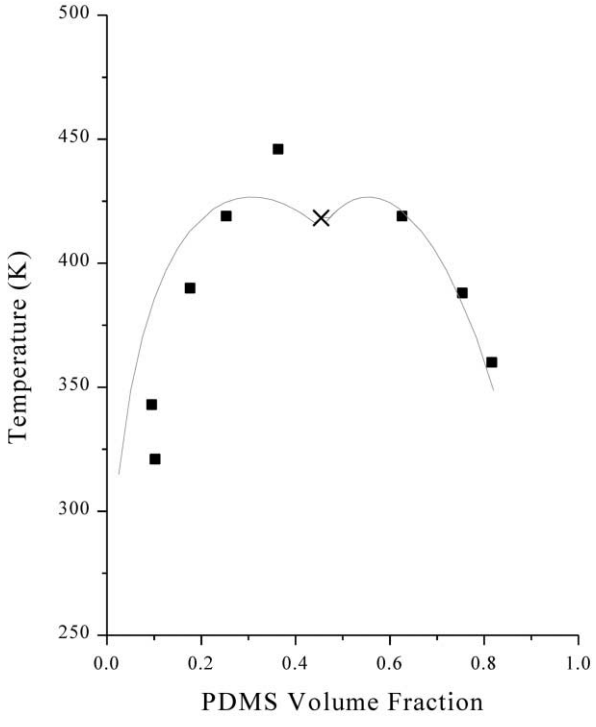

Fig. 5. PIP/PDMS-1310–NH_2 cloud point curves: experimental (squares), binary model (line), critical point (×).

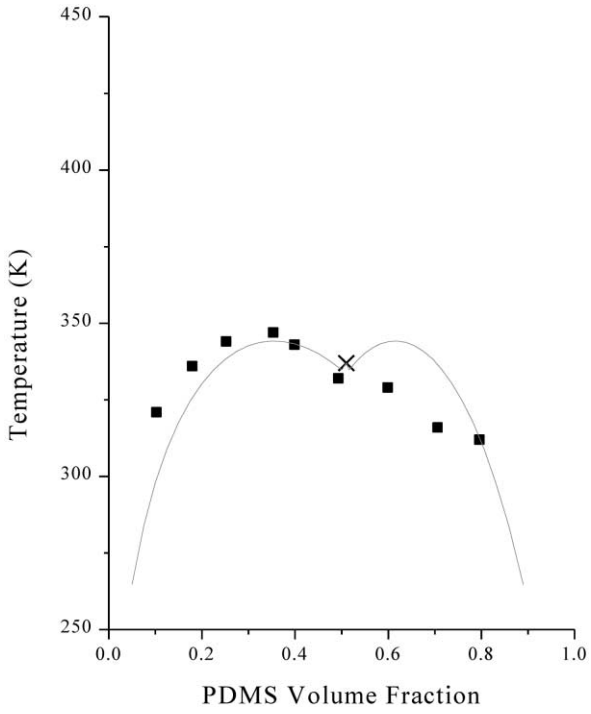

Fig. 6. PIP/PDMS-860–NH_2 cloud point curves: experimental (squares), binary model (line), critical point (×).

for PIP/PDMS–CH_3 blends. This behavior is, at first, unexpected since the interactions of the polar end groups and the non-polar PIP should be unfavorable and repulsive. The absence of any specific attractive interactions between PIP and the amine end groups is supported by the absence of surfactant behavior of PDMS–NH_2 at the PIP/PDMS–CH_3 interface. In fact, binary interactions among the three blend constituents (PIP, PDMS, and the amine end group) should all be unfavorable and repulsive. Although it is possible for the amine or carboxylic acid end groups to exhibit some tendency for aggregation (e.g. carboxylic acids are known to form dimers [28]), especially in the presence of adventitious water, this effect would not be expected in the current system to increase overall blend miscibility. The large magnitude of the interaction parameter, χ_H, is related to the use of a large reference volume.

Table 3
Interaction parameter determined from the regression of experimental cloud point curves for PIP/PDMS blends (based upon a references volume of 128 cm^3/mol)

Blend	χ_H	$\chi_{30°C}$
PIP/PDMS-1270–CH_3[a]	86	0.284
PIP/PDMS-1310–NH_2[b]	53	0.175
PIP/PDMS-890–CH_3[a]	85	0.280
PIP/PDMS-860–NH_2[b]	51.7	0.171

[a] Calculated from the binary F–H model with a temperature-dependent interaction parameter.
[b] Calculated from the F–H model with quasi-binary modification and with a temperature dependent interaction parameter.

The lack of any rigorous theories that take into account the molecular architecture of blends with end-functional homopolymers renders direct interpretation of the experimental results difficult. It is, however, possible to gain considerable insight into the general phase behavior of such systems by consideration of the composite effect of mutually repulsive interactions. As a first order approximation, we consider blends containing end-functional polymers to be analogous to binary blends of a homopolymer and a random copolymer [6]. That is, the end-functional polymer component is approximated as a random copolymer with the relative 'copolymer' composition determined by the volume fraction of end groups. This analogy is particularly useful since the phase behavior of blends of homopolymer/random copolymer has been treated previously by a number of authors, with considerable success in explaining the phase behavior of several important polymer systems [29–31]. The basis of these theories, the binary interaction theory, was first introduced for copolymer–solvent systems [32,33] and then later extended to the case of binary blends of homopolymer/random copolymer [7–9]. In both cases, miscibility was observed to increase, without specific interactions, as the intrachain repulsion of the two repeat units of the copolymer increased.

In the binary interaction theory, the total interaction parameter (χ_{blend}) of a blend of a homopolymer (component 1) and a random copolymer (components 2 and 3) are related to the three binary interaction parameters between individual components as follows:

$$\chi_{blend} = y\chi_{13} + (1-y)\chi_{12} - y(1-y)\chi_{23} \quad (2)$$

where y is the fraction of component 3 in the copolymer. The theory can be simply extended to blends with an end-functional polymer by treating component 3 as the end group and y as the end group volume fraction, calculated directly from the experimentally determined molecular weight and density information. According to Eq. (2), the total interaction parameter (χ_{blend}) decreases if the repulsive interaction between the end group and its polymer backbone (χ_{23}) is greater than the repulsive interaction between the end group and the other homopolymer (χ_{13}). Eq. (2) suggests that overall blend miscibility can be improved by the incorporation of an end group that has a stronger repulsion with its own polymer backbone component that with the other homopolymer.

This hypothesis can be tested by calculating the binary interaction parameters in Eq. (2) through a group additivity approach [34], and comparing these values to the experimental interaction parameters for PIP/PDMS–NH_2 blends determined from model fits. In some of the calculations, an average of the experimentally determined $\chi_{PIP/PDMS-CH_3}$ values, obtained from the F–H model fits of cloud point data, is used in place of $\chi_{PIP/PDMS}$ to calculate the solubility parameter of poly(isoprene) (δ_{IP}). This is primarily due to the extremely wide range of reported solubility parameter values for PIP found in literature (7.4–10.0 $cal^{1/2}\,cm^{-3/2}$) [35]. The calculated interaction parameters and those from model fits of the experimental cloud point data at a temperature of 30°C are presented in Table 4.

Comparison of the experimental and the calculated values of $\chi_{PIP/PDMS\text{-}1310NH_2}$ and $\chi_{PIP/PDMS\text{-}860NH_2}$ reveal relatively good agreement between analogous values. The following trend is evident in the analysis of the intra- and intermolecular binary interaction parameters: $\chi_{DMS/NH2} > \chi_{IP/DMS} > \chi_{IP/NH2}$ (or $\chi_{23} > \chi_{12} > \chi_{13}$). This trend is completely consistent with the expected solubility parameter relationship: $\delta_{NH2} > \delta_{IP} > \delta_{DMS}$. More importantly, this trend is consistent with the concept that the increased miscibility in the functional blends is caused by the large repulsive interaction between the PDMS backbone and the amine end groups, and not by an attractive interaction between the PIP and PDMS.

The lack of strict quantitative agreement between experimental and calculated interaction parameters can be attributed to a variety of different factors. The solubility parameters and molar attraction constants necessary for the group contribution calculations are a clear source of error in the calculations, as they vary widely from source to source. In addition, we assume that the binary interaction theory for random copolymers can represent the enthalpic interactions in end-functional polymers. The theory inherently applies the mean-field approximation, which

Table 4
Calculated and experimental interaction parameters at 30°C

Interacting components	Experimental	Calculated method 1[a]	Calculated method 2[b]	Calculated method 3[c]
PIP/PDMS-1310–NH_2	0.175	0.094	0.144	0.162
PIP/PDMS-860–NH_2	0.171	0.065	0.105	0.129
PIP/PDMS	0.282[d]	0.212	–	–
PDMS/NH_2	–	0.407	0.407	0.285
PIP/NH_2	–	0.032	0.011	6×10^{-6}

[a] Calculated using group additivity approach (dispersive + polar + h-bonding) for δ_{IP} (8.17 $cal^{1/2}\,cm^{-3/2}$), δ_{DMS} (7.17 $cal^{1/2}\,cm^{-3/2}$), and δ_{NH_2} (8.56 $cal^{1/2}\,cm^{-3/2}$).

[b] Using the group additivity values for δ_{DMS} and δ_{NH_2}, and experimentally determined $\chi_{PIP/PDMS-CH_3}$ to calculate δ_{IP} (8.33 $cal^{1/2}\,cm^{-3/2}$).

[c] Using the group additivity values for δ_{NH_2}, an average value of the literature range for δ_{DMS} (7.4 $cal^{1/2}\,cm^{-3/2}$), and experimentally determined $\chi_{PIP/PDMS-CH_3}$ to calculate δ_{IP} (8.55 $cal^{1/2}\,cm^{-3/2}$).

[d] Using experimentally determined $\chi_{PIP/PDMS-CH_3}$ value.

assumes that the chemically distinct blend components are distributed randomly throughout the system. We therefore ignore possible effects of concentration fluctuations and correlation holes due to end group association. These effects are expected to occur on a molecular size scale, do not give rise to scattering of light, and therefore are not observed in our experiments. The existence of these kinds of concentration fluctuations, however, has been confirmed by small-angle X-ray and small-angle neutron scattering studies of liquid macromolecules with heavy atom labels [36], partially labeled homopolymer melts [37], and block copolymers [38,39]. A more rigorous theory, for example based upon the random phase approximation [36], could possibly incorporate these effects but is not currently available.

There are also limitations in the models that we have employed to represent the free energies of the systems studied. The quasi-binary model 'splits' the polydisperse component into two monodisperse fractions in a manner that does not necessarily conserve the overall concentration of end groups. Coupled to this possible limitation is the fact that the quasi-binary model inherently assumes that the interactions of the 2a and 2b components are identical ($\chi_{12a} = \chi_{12b} = \chi_{12}$) and that there are no interactions between them ($\chi_{2a2b} = 0$). Despite the limitations mentioned herein, it should be emphasized that the experimental and calculated interaction parameters displayed in Table 4 quantitatively show good agreement and qualitatively display excellent trends, supporting the previous hypothesis that the observed compatibilization effect of end groups in our blend systems can be attributed to the repulsive interaction between the polymer backbone and its own end group.

Only a few previous studies [10–13] have considered the effects of end groups on the phase behavior of polymer blends. The findings of most of these authors are consistent with the effects of end groups on the thermodynamics of polymer blends observed in the current paper and reported previously by our group [1–6]. The study by Kuo and Clarson [12] examined the phase behavior (i.e. UCST cloud points) of α,ω-trimethylsilyl-terminated PMPS blended with either α,ω-hydroxyl-terminated PDMS (PDMS–OH) or α,ω-trimethylsilyl-terminated PDMS (PDMS–CH_3) and found that the interaction density parameters determined from the analysis of the cloud point data did not change when the PDMS trimethylsilyl end groups were substituted with hydroxyl groups. Their result is consistent with our own observations and with the expectations of the binary interaction theory as well. In a previous study of the surface tension behavior of a variety of α,ω-terminated PDMS materials [1], it was observed that materials with Si–OH termination gave surface tensions that were independent of the molecular weight. Calculations from the group additivity approach demonstrated that the observed behavior could be attributed to the fact that the surface tension of the PDMS backbone and the Si–OH end group were of comparable value. Since surface tension can be related to the solubility parameter, this observation suggests that the solubility parameters of the Si–OH end group and the PDMS backbone are also of comparable value, and leads to the conclusions that $\chi_{23} \cong 0$, and that $\chi_{13} = \chi_{12}$ for PMPS/PDMS–OH blends. The overall interaction density parameters of the PMPS/PDMS–OH and PMPS/PDMS–CH_3 blends, according to Eq. (2), are therefore predicted to be comparable, consistent with the experimental findings presented in Ref. [12].

4. Conclusions

Cloud point curves determined by laser light scattering demonstrate that functional end groups can have a profound influence on the phase behavior of low molecular weight polymer blends manifesting upper critical solution temperatures. The incorporation of end groups that have repulsive interactions with both blend homopolymers leads to increased miscibility as indicated by a reduction in the upper critical solution temperature. This effect occurs when the relative repulsion between an end group and the polymer chain it is attached to is greater than that between the end group and the second polymer. The phase diagrams for the end-functional blends can be nearly quantitatively accounted for by the modified Flory–Huggins–Staverman lattice models that employ binary interaction theory and group additivity concepts to calculate the effect of end groups on the enthalpy of interactions.

Acknowledgements

This research was supported in part by grants from the Office of Naval Research, the National Science Foundation Polymer Program (DMR-8818232 and DMR-9710265), and the University of Connecticut Polymer Compatibilization Consortium. One of the authors (C.A.F.) acknowledges support from a State of Connecticut Department of Higher Education High Technology Fellowship. The authors thank Dr Judith Riffle (VPI) and Dr Iskender Yilgor (Goldschmidt) for supplying some of the samples, and Dr Val Krukonis (Phasex Corp.) for his help in fractionating some of the materials.

Appendix A. Description of the quasi-binary model

In addition to the F–H rigid lattice model, which is only applicable to binary mixtures, a quasi-binary model, described originally by Koningsveld et al. [17,19] for a polymer–solvent system, was used in the current paper to better simulate the overall phase behavior of the polydisperse PDMS–NH_2 components. A brief description of the model, the calculation method and the utilized pertinent equations are provided here.

In the calculation of the quasi-binary model, the polydisperse component (polymer 2) is treated as a mixture of two monodisperse homopolymer fractions (species 2a and 2b) as a zero order approximation. Using an analogous method of derivation as the F–H model, the modified governing equation for the quasi-binary system becomes:

$$\frac{\Delta G}{NRT} = \frac{\phi_1}{r_1}\ln(\phi_1) + \frac{\phi_{2a}}{r_{2a}}\ln(\phi_{2a}) + \frac{\phi_{2b}}{r_{2b}}\ln(\phi_{2b}) + \chi_{12}\phi_1(\phi_{2a} + \phi_{2b}) \quad \text{(A1)}$$

where $\phi_{2a} + \phi_{2b} = \phi_2$ and $\phi_1 + \phi_2 = 1$. In the above equations, ϕ_i denotes the volume fraction of species i, r_i is the relative molar volume, or chains length, T is the absolute temperature, R is the gas constant, and χ_{12} denotes the familiar F–H interaction parameter. Note that all molar volumes (r) and interaction parameters (χ) used in the modeling programs were calculated with respect to the reference volume of a dimethylsilylpropylamine end group (denoted simply as NH_2).

Within this model, the effect of molecular weight distribution on the phase behavior of a quasi-binary blend is taken into account in determining the characteristics of the two monodisperse fractions of polymer 2. The relative molar volumes (r_{2a} and r_{2b}) and weight fractions (w_{2a} and w_{2b}) of the new species can be directly calculated using the experimentally-determined number-average (r_n), weight-average (r_w), and z-average (r_z) relative molar volumes of the polydisperse component by solving simultaneously the following equations:

$$w_{2a} + w_{2b} = 1 \quad \text{(A2)}$$

$$\frac{w_{2a}}{r_{2a}} + \frac{w_{2b}}{r_{2b}} = \frac{1}{r_n} \quad \text{(A3)}$$

$$w_{2a}r_{2a} + w_{2b}r_{2b} = r_w \quad \text{(A4)}$$

$$w_{2a}r_{2a}^2 + w_{2b}r_{2b}^2 = r_w r_z \quad \text{(A5)}$$

It is important to note that the miscibility envelope, as represented by the cloud point curve, of quasi-binary systems does not coincide with the binodal, which represent the coexisting phase compositions at given temperatures. In the case of a simple binary mixture, the cloud point curve coincides with the binodal and the two branches of the curve represent coexisting phases. In the quasi-binary system, however, the determination of the cloud point curve involves calculation of the incipient or 'shadow' curve, which is a cross-section of the three-dimensional ternary phase diagram at a constant relative composition ratio between species 2a and 2b in the newly formed phase. Schematically, this is illustrated well by Figs. 2 and 3 in Ref. [17] and Figs. 1, 2 and 4 in Ref. [19], and is mathematically performed using Eq. (A11) or Eq. (A12). As in normal ternary systems, the chemical potential equations of the three individual species Eqs. (A6)–(A8) for the two coexisting phases (α and β) are equated to produce the phase diagram: $\Delta\mu_1^\alpha = \Delta\mu_1^\beta$, $\Delta\mu_{2a}^\alpha = \Delta\mu_{2a}^\beta$, and $\Delta\mu_{2b}^\alpha = \Delta\mu_{2b}^\beta$.

$$\frac{\Delta\mu_1}{r_1RT} = \frac{\ln(\phi_1)}{r_1} + \left(\frac{1}{r_1} - \frac{1}{r_{2a}}\right)\phi_{2a} + \left(\frac{1}{r_1} - \frac{1}{r_{2b}}\right)\phi_{2b} + \chi_{12}(\phi_{2a} + \phi_{2b})^2 \quad \text{(A6)}$$

$$\frac{\Delta\mu_{2a}}{r_{2a}RT} = \frac{\ln(\phi_{2a})}{r_{2a}} + \left(\frac{1}{r_{2a}} - \frac{1}{r_1}\right)\phi_1 + \left(\frac{1}{r_{2a}} - \frac{1}{r_{2b}}\right)\phi_{2b} + \chi_{12}\phi_1^2 \quad \text{(A7)}$$

$$\frac{\Delta\mu_{2b}}{r_{2b}RT} = \frac{\ln(\phi_{2b})}{r_{2b}} + \left(\frac{1}{r_{2b}} - \frac{1}{r_1}\right)\phi_1 + \left(\frac{1}{r_{2a}} - \frac{1}{r_{2b}}\right)\phi_{2b} + \chi_{12}\phi_1^2 \quad \text{(A8)}$$

Other relations necessary in the calculation of the quasi-binary phase diagram include:

$$\phi_1^\alpha + \phi_{2a}^\alpha + \phi_{2b}^\alpha = 1 \quad \text{(A9)}$$

$$\phi_1^\beta + \phi_{2a}^\beta + \phi_{2b}^\beta = 1 \quad \text{(A10)}$$

$$\frac{\phi_{2b}^\alpha}{\phi_{2a}^\alpha} = \frac{w_{2b}}{w_{2a}} \quad \text{(A11)}$$

$$\frac{\phi_{2b}^\beta}{\phi_{2a}^\beta} = \frac{w_{2b}}{w_{2a}} \quad \text{(A12)}$$

As mentioned previously in the paper, the location of the critical point is also remarkably affected by the molecular weight distribution of the blend components. It has been shown by previous authors [17–19,25] that the 'true' critical point of liquid–liquid multicomponent polymer solutions is located on the right-hand branch of the CPC, often accompanied by a depression at the location. In addition, these authors demonstrated that the specific features of this depression are largely dependent on the details of the molecular weight distribution, with the depression deepening with the increasing M_z/M_w at constant M_w/M_n. Due to the double critical point phenomena observed in the cloud point curves of quasi-binary systems, it becomes difficult to approximate the location of the true critical point graphically, as is possible in strictly binary systems. The true critical point can be calculated using Eqs. (A15) and (A16), which are derived. using the strict thermodynamic definition of the critical point (Eqs. (A13) and (A14)).

$$\begin{vmatrix} \partial J_s/\partial\phi_{2a} & \partial J_s/\partial\phi_{2b} \\ \partial^2(\Delta G/NRT)/\partial\phi_{2b}\partial\phi_{2a} & \partial^2(\Delta G/NRT)/\partial\phi_{2b}^2 \end{vmatrix} = 0 \quad \text{(A13)}$$

$$J_s = \begin{vmatrix} \partial^2(\Delta G/NRT)/\partial\phi_{2a}^2 & \partial^2(\Delta G/NRT)/\partial\phi_{2a}\partial\phi_{2b} \\ \partial^2(\Delta G/NRT)/\partial\phi_{2b}\partial\phi_{2a} & \partial^2(\Delta G/NRT)/\partial\phi_{2b} \end{vmatrix} \tag{A14}$$

$$\phi_{2,\text{critical}} = \frac{1}{1+\sqrt{\dfrac{r_w^2}{r_1 r_z}}} \tag{A15}$$

$$\chi_{\text{critical}} = \frac{1}{2}\left(\frac{1}{\sqrt{r_1}} + \frac{1}{\sqrt{r_w}}\right)^2 \tag{A16}$$

References

[1] Jalbert CJ, Koberstein JT, Yilgor I, Gallagher P, Krukonis V. Macromolecules 1993;26:3069.
[2] Jalbert CJ, Koberstein JT, Balaji R, Bhatia QS, Salvati Jr. L, Yilgor I. Macromolecules 1994;27:2409.
[3] Elman JF, Johs BD, Long TE, Koberstein JT. Macromolecules 1994;27:5341.
[4] Mason R, Jalbert CJ, Gunesin B, Koberstein JT. Advances in Colloid and Interface Chemistry (accepted for publication).
[5] Fleischer CA, Morales AR, Koberstein JT. Macromolecules 1994;27:379.
[6] Fleischer CA, Koberstein JT, Krukonis V, Wetmore P. Macromolecules 1993;26:4172.
[7] ten Brinke G, Karasz F, MacKnight WJ. Macromolecules 1983;16:1827.
[8] Kambour R, Bendler JT, Bopp RC. Macromolecules 1983;16:753.
[9] Paul DR, Barlow JW. Polymer 1984;25:487.
[10] Callaghan TA, Paul DR. Macromolecules 1993;26:2439.
[11] Kollodge JS, Porter RS. Macromolecules 1995;28:4097.
[12] Kuo CM, Clarson SJ. Eur Polym J 1993;29:661.
[13] Qian C, Grigoras S, Kennan L. Macromolecules 1996;29:1260.
[14] Yilgor I, McGrath JE. Adv Polym Sci 1988;86:1.
[15] Elsbernd CS, Spinu M, Krukonis VJ, Gallagher PM, Mohanty DK, McGrath JE. Adv Chem 1990;224:145.
[16] Flory PJ. Principles of polymer chemistry. Ithaca, NY: Cornell University Press, 1953.
[17] Koningsveld R, Staverman AJ. J Polym Sci Part A2 1968;6:305.
[18] Koningsveld R, Staverman AJ. J Polym Sci Part A2 1968;6:349.
[19] Koningsveld R, Staverman AJ. Kolloid Z Z Polym 1967;218:114.
[20] Gordon M, Chermin HAG, Koningsveld R. Macromolecules 1969;2:207.
[21] Kennedy JW, Gordon M, Koningsveld R. J Polym Sci Part C 1972;39:43.
[22] van Opstal L, Koningsveld R, Kleintjeins LA. Macromolecules 1991;24:221.
[23] Koningsveld R, Kleintjens LA, Leblans-Vinck AM. J Phys Chem 1987;91:6423.
[24] Solc K. Macromolecules 1970;3:665.
[25] Koningsveld R, Staverman AJ. J Polym Sci Part A2 1968;6:325.
[26] Staverman AJ. Recl Trav Chim 1937;56:885.
[27] Bondi A. J Phys Chem 1964;68:441.
[28] MacKnight WJ, McKenna LW, Read BE, Stein RS. J Chem Phys 1968;72:1122.
[29] Ellis TS. Macromolecules 1989;22:742.
[30] Ellis TS. Macromolecules 1991;24:3845.
[31] Zhu KJ, Chen SF, Ho T, Pearce EM, Kwei TK. Macromolecules 1990;23:150.
[32] Simha R, Branson H. J Chem Phys 1944;12:253.
[33] Stockmayer WH, Moore Jr. LD, Fixman M, Epstein BN. J Polym Sci 1955;16:517.
[34] Jalbert CJ, Koberstein JT, Hariharan A, Kumar SK. Macromolecules 1997;30:4481.
[35] Brandrup J, Immergut EH. Polymer handbook. 3rd ed. New York: Wiley Interscience, 1989.
[36] de Gennes PG. J Phys 1970;31:235.
[37] Leibler L, Benoit H. Polymer 1981;22:195.
[38] LeGrand AD, LeGrand DG. Macromolecules 1979;12:450.
[39] Owens JN, Gancarz IS, Koberstein JT, Russell T. Macromolecules 1989;22:3380.